EurJIC
European Journal of Inorganic Chemistry

Research Article
doi.org/10.1002/ejic.202200225

Chemistry Europe
European Chemical Societies Publishing

www.eurjic.org

VIP *Very Important Paper*

Synthesis of Triple-Stranded Diruthenium(II) Compounds

Kate L. Flint,[a] David M. Huang,[a] Oliver M. Linder-Patton,[a] Christopher J. Sumby,[a] and F. Richard Keene*[a]

A series of ligands containing a 1,4-disubstituted 1,2,3-triazole unit have been used for the formation of triple-stranded dinuclear Ru(II) complexes. In contrast to the previously reported complexes of labile metals, the use of inert Ru(II) enabled stereoisomeric mixtures of triple-stranded diruthenium(II) complexes to be accessed. The chromatographic resolution of the enantiomers of a reported helicate containing a more rigid 1,4-xylyl spacer was carried out on cellulose. The ligand spacer was modified and as the flexibility increased the production of isomeric mixtures was detected; the mesocate and helicate forms were separated when an *n*-propyl spacer was used. This pair of diastereomers was found to exhibit photoconversion, a unique observation for Ru(II) compounds of this type. Partial separation via chromatographic resolution was achieved for compounds containing an *n*-butyl spacer, and the presence of a mesocate/helicate pair confirmed.

Introduction

The persistent presence of the helical motif in biology (in polypeptides, nucleic acids, proteins, enzymes etc.) gives rise to the possibility that artificial helical molecules, like metallohelicates, may have potential in therapeutic applications.[1] Alternatively, these molecules could be used to probe the mechanisms of biological interactions, as analogues of the helical motifs are present in biological molecules.

There has been interest in the biological efficacy of ruthenium complexes as anti-tumour,[2] antimicrobial,[3] anti-parasitic[4] and anti-fungal agents,[5] and we were interested in developing helical species containing ruthenium centres. The ruthenium(II) metal centre is octahedral, and the simplest di-metallic helical structure will necessarily be a double-stranded helix should di(tridentate) ligands by employed, or triple-stranded for di(bidentate) ligands (see Figure 1). In both cases there is also the possibility of a mesocate diastereoisomer.

The earliest report of a homonuclear ruthenium helicate was by Crane and Sauvage, utilising a di(tpy)-based ligand to form a double-stranded assembly.[6] Following this a triple-stranded species was reported by Pascu *et al.*, synthesising a diruthenium(II) helicate from di(pyridylimine) ligands in 1% yield after extensive purification.[7] The ability of the Ru(II) compound to bind and coil DNA was demonstrated, as well as anti-cancer and anti-viral activity.[8] Subsequently, Glasson *et al.*

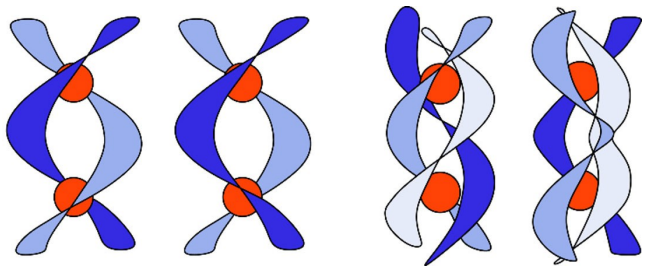

Figure 1. Schematic representations showing the chiral helicate and achiral mesocate for double-stranded (LEFT) and triple-stranded (RIGHT) assemblies.

employed a quaterpyridine ligand to synthesise a triple-stranded ruthenium helicate.[9] In this approach a significantly higher yield of 36% was attained, and the chromatographic resolution and DNA binding of the different enantiomers studied. More recently, Kumar *et al.* have synthesised a triple-stranded ruthenium helicate and explored the anti-bacterial properties, describing activity against both Gram positive and Gram negative bacteria as "extremely modest".[10]

In all of these cases a single helicate product was obtained, and the first Ru(II) helicate/mesocate pair was only recently reported by Allison *et al*, incorporating di(thiazole-bipyridine) ligands, for which the diastereomers were chromatographically separated and the anti-cancer activity of these compounds assessed, showing promising selectivity and cytotoxicity.[11] Since this initial study, we have reported the synthesis and separation of an additional pair of Ru(II) double-stranded diastereomers.[12]

In general, mesocates are less commonly found than helicates in the literature, with the first X-ray structure of a mesocate only reported in 1995 by Albrect and Kotila.[13] Since that time, several helicate/mesocate mixtures have been observed in solution, with Zhang and Dolphin reporting the first separation of a pair of helicate/mesocate diastereomers in 2009.[14] The ability to influence the formation of the chiral helicate or achiral mesocate has become a point of considerable

[a] *Dr. K. L. Flint, Dr. D. M. Huang, Dr. O. M. Linder-Patton, Prof. C. J. Sumby, Prof. F. R. Keene*
Department of Chemistry,
School of Physical Sciences,
University of Adelaide,
Adelaide, S.A. 5005, Australia
E-mail: richard.keene@adelaide.edu.au

Supporting information for this article is available on the WWW under https://doi.org/10.1002/ejic.202200225

Research Article
doi.org/10.1002/ejic.202200225

interest, with careful ligand design[15] and anion binding[16] being employed in attempts to control product distribution, with the mixture being monitored by chromatographic separation.[11–12,14]

Ligands containing 1,4-disubstituted 1,2,3-triazole units have been used in the synthesis of a wide variety of supramolecular assemblies, most notably by Crowley and co-workers,[17] including for the formation of dinuclear helicates and mesocates.[10,18] Initially, Vellas *et al.* showed that $[Fe_2L_3]^{2+}$ triple-stranded helicates could be formed from the assembly of Fe(II) and an extensive family of bis-2-(1-*R*-1*H*-1,2,3-triazol-4-yl) ligands.[19] This family of ligands was further explored by Wu *et al.* by varying the shape and size of the spacer moiety, producing dinuclear compounds containing Zn(II), Ni(II), and Fe(II).[20] The authors found that while all linkers assembled to form discrete triple-stranded compounds other factors affected whether a helicate or mesocate, or mixture of both, resulted. Specifically, the orientation of the lone pairs on the non-coordinated nitrogen of the triazole, which point towards the interior of the assembled structure, destabilise the compounds when short spacers are present, driving the formation of larger assemblies. The length and flexibility of the spacer was also crucial, following the selection rules for 2,2'-bipyridine and catechol-based systems[21] in which ligands containing an odd-numbered spacer (for example an *n*-propyl chain) led to the formation of mesocates, whereas for even-numbered spacers helicates were favoured. However, the authors noted that once the chain length reached C_5 (*n*-pentyl) a mixture of isomers was observed.

The Fe(II) complexes described above have been trialled in biological settings; however, the applications of these are limited by their poor stability in biological media.[19] To improve stability, Ru(II) analogues,[22] including a triple-stranded helicate,[10] have been synthesised, although no attempts to resolve these chiral assemblies have been reported.

Based on these findings, in this work a series of ligand spacers (see Figure 2) of varying bulk and flexibility were selected as potential candidates for the synthesis of diruthenium(II) compounds. While the Fe(II) analogues had been reported to follow the odd/even rules of helicate/mesocate formation,[19–20,23] it was proposed that by using the relatively inert Ru(II) node it may be possible to break these rules and obtain alternative kinetically preferred products, rather than the thermodynamically preferred option as in the previous cases where labile metal centres were involved.

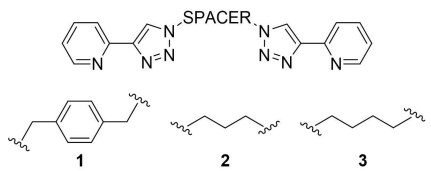

Figure 2. Ligands used for the synthesis of Ru(II) complexes, showing the general ligand structure and specific spacer functionality.

Results and Discussion

Using a 1,4-xylyl spacer ligand (1)

The synthesis of a triple-stranded Ru(II) helicate species $[Ru_2(\mu\text{-}\mathbf{1})_3]^{4+}$ utilising the ligand (**1**) containing the 1,4-xylyl spacer was undertaken following the procedures outlined by Kumar *et al.*[10] The $[Ru_2(\mu\text{-}\mathbf{1})_3]^{4+}$ helicate product was verified by 1D and 2D NMR spectroscopy and single crystal X-ray diffraction (SCXRD).

Resolution of helicate

While the synthesis of a number of related supramolecular assemblies incorporating the 1,4-xylyl spacer ligand (1) have been reported,[10,17b,18–20,23–24] there is no record of attempts to resolve any of the helicates. Because of the potential interest in probing the enantiospecific interactions of these types of compounds with biological substrates, resolution of the triple-stranded Ru(II) helicate was pursued. Based on the resolution achieved on a cellulose stationary phase for a number of triple-stranded helicates by Hannon and co-workers,[25] resolution of the helicate $[Ru_2(\mu\text{-}1)_3]^{4+}$ was initially attempted using chromatography on a cellulose support with NaCl eluent solutions of varying concentrations. Optimal separation was achieved for [NaCl] = 2 M, where a portion of yellow compound was found to elute (F1), while the remainder was smeared down the length of the column. This second fraction (F2) could be removed by subsequent elution with 0.5 M sodium 4-toluenesulfonate, or 20% acetone/2 M NaCl. Circular dichroism analysis of the two fractions (in CH_3CN solution, once exchanged by anion metathesis to their respective PF_6^- salts by addition of KPF_6 to the eluate samples) revealed equal and opposite CD responses when normalised for concentration (see Figure 3) with the highest magnitude of 157 $M^{-1}cm^{-1}$ at ~276 nm.

The two fractions were further examined using NMR and UV-VIS spectroscopy and found to have identical spectra.

Crystals of neither of the enantiomeric forms of $[Ru_2(\mu\text{-}\mathbf{1})_3]^{4+}$ could be obtained, and so the configurations of the fractions F1

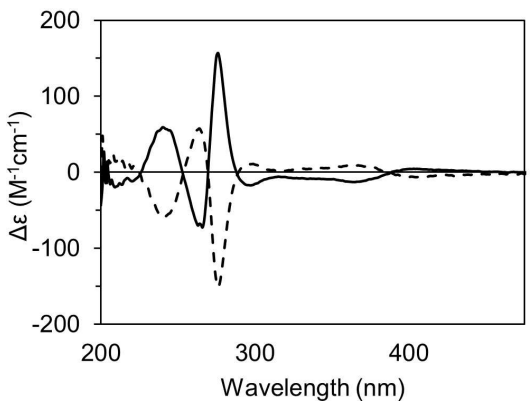

Figure 3. CD spectra of $[Ru_2(\mu\text{-}\mathbf{1})_3]^{4+}$ resolved on cellulose: F1 (—) refers to the first eluting fraction (aq. 2 M NaCl); F2 (- - - -) refers to the second eluting fraction (eluted with 20% acetone/2 M NaCl).

and F2 were tentatively assigned based on comparison of CD spectra with mononuclear species with analogous tris(bidentate)ruthenium coordination motifs with polypyridyl ligands: based on the configurational assignments for $[Ru(phen)_3]^{2+}$ (phen = 1,10-phenanthroline) and $[Ru(bpy)_3]^{2+}$ (bpy = 2,2′-bipyridine) by McCaffery *et al.*[26] F1 was assigned as the configuration as the *M*-helicate (ΛΛ), and F2 as the *P*-helicate (ΔΔ). This assignment was in agreement with that reported by Glasson *et al.* for the resolved triple-stranded helicate containing quaterpyridine ligands, where there were similarities in the direction of the Cotton effects for each enantiomer.[9]

Presence of a secondary product

While in the majority of microwave syntheses a single product was present based on the crude NMR spectrum, on occasion a secondary set of peaks was observed, with analogous chemical shifts and integrations to the helicate peaks (see Figure S1). Interestingly, in the original synthesis of the helicate Kumar *et al.* made no mention of a secondary product.[10]

The relationship of this unknown compound to the helicate was probed by diffusion-ordered (DOSY) NMR experiments: comparison of the diffusion coefficients for the two sets of peaks revealed them to be the same size (see Figure S2), suggesting that this second species was another dinuclear compound – possibly a mesocate or some other Ru_2L_3 assembly.

Separation of the two species was attempted by fractional crystallisation methods, with addition of $NaBF_4$ to an aqueous solution of the Cl^- salt of the crude product. It was found that the pure helicate could be isolated from the reaction mixture, precipitating as the BF_4^- salt, while a mixture of the helicate and the unknown component remained in solution (see Figure S3). The pure unknown compound was not able to be isolated by this method.

The variation of the reaction conditions to control the initial product distribution was investigated, and this investigation revealed that the relative ratio of helicate to the secondary product increased with longer reaction time (see Figure S4). However, the secondary species did not always appear in the crude product mixture, with some syntheses yielding only helicate (in agreement with the earlier reports of Kumar *et al.*).[10] As such, the secondary product was not investigated further, but may represent the corresponding mesocate species.

Using an *n*–propyl spacer ligand (2)

The synthesis of an analogous triple-stranded Ru(II) compound utilised the 1,3-bis{4-(pyridine-2-yl)-1*H*-1,2,3-triazol-1-yl}propane ligand (**2**)[27] under the same microwave conditions used for $[Ru_2(\mu\text{-}\mathbf{1})_3]^{4+}$ above. It was anticipated that the $[Ru_2(\mu\text{-}\mathbf{2})_3]^{4+}$ product would favour formation of the mesocate; however, characterisation by ^{13}C NMR spectroscopy revealed the presence of two products. In the ^{13}C NMR spectrum many of the signals were overlapping (see Figure S5 and Figure S6), and when this was accounted for 18 signals could be identified in total. The notion of two separate products was supported by 2D HSQC NMR studies, with the complicated multiplets appearing at 4.5 and 2.6 ppm belonging to the *n*-propyl spacer hydrogens coupled to separate carbon signals (see Figure S7).

The ^1H NMR spectrum of the Cl^- salt in D_2O also showed the presence of the two species (see Figure S8). The PF_6^- salt (in CD_3CN) and the Cl^- salt (in D_2O) were found to be thermally stable over a period of seven days at 50 °C, with no changes in chemical shift or relative integration of the signals, ruling out degradation of the initial product as the source of the secondary species (see Figure S9 and Figure S10). The relationship of the two species was probed by DOSY NMR spectroscopy, using a sample of the crude mixture as the Cl^- salt in D_2O. Across the spectrum all signals corresponded to compounds with a similar diffusion coefficient (see Figure S11), suggesting that both were of a similar size, likely two dinuclear species.

Further experiments were conducted in a range of solvents using the crude product as either the PF_6^- or Cl^- salts and fortuitously it was observed that for the Cl^- salt the sample was partially soluble in d_6-DMSO: the soluble portion contained predominantly one species by ^1H NMR spectroscopy, while the remaining DMSO-insoluble portion was dissolved in D_2O and found to contain the second species. The two species were fully separated after two washes with DMSO, and when converted to the PF_6^- salts each showed a single set of resonances by ^1H NMR spectroscopy and only nine resonances by ^{13}C NMR (see Figure 4). Upon examination of the ^{13}C NMR spectra of the purified species it was seen that many resonances were highly overlapping in the aromatic region, but in the upfield region the multiplets for the hydrogens on the *n*-propyl spacer resolved into separate signals at 4.4 and 2.5 ppm. Intriguingly, the *n*-propyl spacer hydrogen signals of the DMSO-soluble compound appeared as a pair of multiplets (4.4 ppm) followed by a quintet (2.5 ppm), whereas for the DMSO-insoluble compound the pattern appeared to be reversed, with a multiplet at 4.4 ppm followed by a pair of multiplets at 2.5 ppm, suggesting that the major differences in chemical environment for these compounds must occur for hydrogens in the *n*-propyl spacer region.

The possibility of the two species being conformers of the expected mesocate was addressed using variable temperature NMR experiments. ^1H NMR spectra were collected at 5° increments, from 25 to 50 °C, for the original mixture as the Cl^- salt in D_2O to monitor changes in the ratio of the two species. Over this temperature gradient, sharpening of the peaks across the aromatic region was observed, but comparison of the relative integration of the two triazole signals showed negligible change, suggesting that two species were unlikely to be conformers (see Figure S12).

Crystals of the two species were grown as the PF_6^- salts, and the structure of each elucidated by SCXRD. The DMSO-insoluble fraction of the Cl^- salt was dissolved in H_2O, and then exchanged to the PF_6^- salt by metathesis. Crystals suitable for X-ray diffraction were grown by vapour diffusion of diisopropyl

Research Article
doi.org/10.1002/ejic.202200225

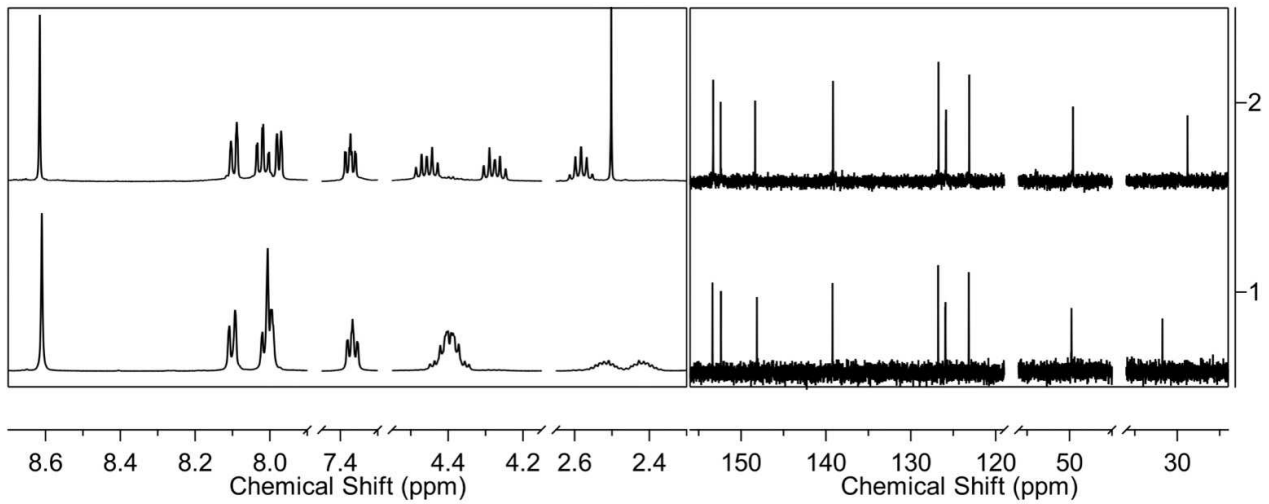

Figure 4. (LEFT) Partial ^{1}H NMR spectra (500 MHz, CD_3CN, 298 K, PF_6^- salt) and (RIGHT) ^{13}C NMR spectra (126 MHz, CD_3CN, 298 K, PF_6^- salt) showing the separated $[Ru_2(\mu\text{-}\mathbf{2})_3]^{4+}$ species: (1) DMSO-insoluble Cl^- salt; (2) DMSO-soluble Cl^- salt. (Peak at 2.5 ppm due to residual DMSO).

ether into a nitromethane solution of the compound, and the resulting structure confirmed the formation of the mesocate of the type $[Ru_2(\mu\text{-}\mathbf{2})_3]^{4+}$ (**4**), shown in Figure 5a. The complex crystallises in the space group $P6_3/m$. Present in the asymmetric unit are one-sixth of a ruthenium(II) mesocate cation, one PF_6^- anion, one nitromethane, and one-third of a potassium cation

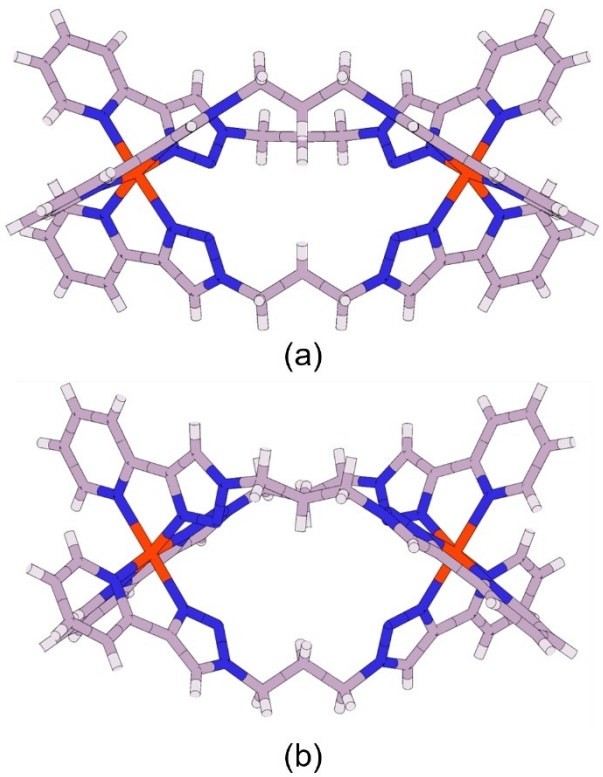

Figure 5. Crystallographic models showing the molecular structure of (a) the purified ruthenium mesocate **4**, and (b) the helicate **5** of $[Ru_2(\mu\text{-}\mathbf{2})_3](PF_6)_4$. Solvent molecules and counter ions have been omitted for clarity.

(remaining from conversion to the PF_6^- salt using KPF_6). The presence of potassium was confirmed by scanning electron microscopy/energy-dispersive X-ray spectroscopy (SEM/EDX) analysis of single and crushed crystals (see Figures S29, S30, S31, and Table S2). The two octahedral ruthenium(II) centres are separated by 10.084(2) Å and bridged by three ligands such that the stereochemistry of the metal centres of each discrete unit is ΛΛ. Inclusion of a van der Waals surface shows a central cavity in the structure due to the spatial orientation of the *n*-propyl spacer (see Figure S25).

To determine the identity of the DMSO-soluble portion of the Cl^- salt, an excess of H_2O was added to a solution of the purified compound as the Cl^- salt in DMSO and the sample exchanged to the PF_6^- salt by metathesis. Crystals suitable for X-ray diffraction were grown by vapour diffusion of diisopropyl ether into an acetonitrile solution of the compound. The resulting structure revealed the formation of a helicate of the type $[Ru_2(\mu\text{-}\mathbf{2})_3]^{4+}$ (**5**), shown as the *P*-helicate in Figure 5b. The complex crystallises in the space group *P*-31*c*. Present in the asymmetric unit are two-thirds of a ruthenium(II) helicate cation and $2^2/_3$ PF_6^- anions. As the helicate has not been resolved, the complex crystallises as a mixture of enantiomers which can be differentiated in the extended crystal structure. In the solid-state adjacent helicates have their pair of octahedral Ru(II) centres separated by different distances, in some molecules the separation in 9.376(4) Å, while in other the metal centres are separated by 8.698(3) Å (see Figure S26). The helicates are packed in interdigitated AB layers with one layer consisting of helicates with a short Ru–Ru distance and one of helicates with alternating short and long Ru–Ru distance. Each long helicate in the lattice is surrounded by six helicates with a short Ru spacing (three in one layer above and three in a layer below). These are both notably shorter than the equivalent distance in the mesocate. Inclusion of a van der Waals surface shows a central cavity similar to that seen for the mesocate, due to the

Research Article
doi.org/10.1002/ejic.202200225

manner in which the ligands wrap around the metal centres (see Figure S27).

The two dinuclear Ru(II) diastereomers containing the *n*-propyl spacer ligand (**2**) showed significant structure variation, aside from the obvious difference in chirality. The mesocate was a slightly longer molecule in terms of the Ru(II)-Ru(II) distance and possessed a central cavity ≈ 17 Å^3. Due to the elongation of the ligands down the sides of the structure, the cavity is composed of two overlapping spheres. The helicate, despite having a shorter inter-ruthenium distance, had a cavity that was larger in volume (≈ 30 Å^3), and was far more cylindrical in shape than that of the mesocate due to the manner in which the ligands wrap round the two metal centres. The volumes of the central cavities of both structures were calculated from the crystal structure using the program MoloVol.[28]

The yellow colour of the helicate and mesocate synthesised using the *n*-propyl spacer ligand (**2**) is typical for Ru(II) complexes containing ligands of this design, with the UV/Vis absorption spectra showing an MLCT band at 382 nm ($\varepsilon_{mesocate}$ $[M^{-1}cm^{-1}] = 2.46 \times 10^4$; $\varepsilon_{helicate}$ $[M^{-1}cm^{-1}] = 3.17 \times 10^4$; see Figure S24).

As further confirmation, the HR ESI-MS of the two dinuclear products showed ions of identical formula masses – *m/z* 300.2222 (corresponding to $\{[Ru_2(\mathbf{2})_3].4PF_6\}$; see Figures S21 and S22).

Isomer distribution

It was proposed that ligand flexibility may be important to facilitate the formation of multiple dinuclear species, in contrast to the single helicate formed from the more rigid 1,4-xylyl spacer ligand described above. Given that both a mesocate (4) and helicate (5) were found to be present using the *n*-propyl spacer ligand, modelling was conducted using density functional theory (DFT) to better understand the product distribution and relative energies of the species. The relative stability of the two isomers was calculated *in vacuo* and in a dielectric medium, using the dielectric constant of acetonitrile (see Table S3). From these results, *in vacuo* the mesocate is a more stable isomer than the helicate ($\Delta E = 19.4$ kJ/mol, and $\Delta G = 24.7$ kJ/mol, respectively). This was also the case in a dielectric medium; however, the difference in stability was greatly decreased (where $\Delta E = 1.6$ kJ/mol, and $\Delta G = 7.0$ kJ/mol). These findings agree with the experimentally observed product distribution, in which both the mesocate and helicate can be isolated in roughly equal proportions. It is proposed that the small difference in stability for the two dinuclear species, combined with the inert nature of the Ru(II) metal centre, allowed isolation of a helicate containing an odd-numbered spacer, a compound not previously accessible using more labile transition metals with this ligand.

Isomerisation

It was observed for the purified diasteroisomers in solution that after hours or days mixtures were persistently visible in samples when analysed by NMR spectroscopy, and given the small difference in their relative energies, the possibility of isomer interconversion was investigated.

Initially samples of the purified helicate and mesocate as the Cl^- salts were either re-exposed to reaction conditions (microwave reactor: 200 W, 200 psi, 225 °C, five hours) or heated in D_2O at 60 °C for seven days: in both cases it appeared that no significant interconversion of the isomers occurred via thermal pathways (see Figures S36, S37, S38, and S39).

Nevertheless, interconversion was observed for purified samples left in solution for hours or days on the bench, and the possibility of light-induced isomerisation was investigated. The samples which had previously undergone heating as the Cl^- salts in D_2O were left in ambient light at room temperature for 30 days, and the NMR spectra collected after this time. For both the mesocate and helicate significant conversion between the two isomers was observed. The interconversion was most clearly seen in the aromatic region, where hydrogen resonances for the purified compound (either mesocate or helicate) diminished, and resonances corresponding to the other isomer emerged (see Figures S40 and S41). In addition, the multiplets corresponding to the *n*-propyl spacer hydrogens at 4.5 and 2.8 ppm greatly increased in complexity, indicating the presence of both dinuclear compounds.

The ability to control the formation of mesocates and helicates has been a topic of great interest since the first reported mesocate structures. While some studies have supported the odd/even mesocate/helicate rule proposed by Albrecht *et al.*[13,15a] there have been some exceptions reported. Interconversion within families of coordination cages – due to anion dependency, host-guest interactions, or post-assembly mediation – has generally been seen for mesocates or helicates converting to larger architectures. These interconversions have been studied for a wide range of metal centres;[29] however, there are far fewer examples of simple mesocate-to-helicate transformations. Goetz and Kruger reported the formation of triple-stranded Fe(II) compounds, where both the helicate and mesocate existed in DMSO as the BF_4^- salts, but when Cl^- ions were introduced conversion to the helicate was favoured.[16a] The authors proposed that the preference for the helicate isomer was likely due to two Cl^- ions being bound within the central cavity of the helicate, which does not occur in the mesocate. Careful selection of anions was also shown by Cui *et al.* to influence the product distribution in iron- and copper-containing compounds, with larger tetrahedral anions favouring mesocate formation, with smaller spherical or trigonal planar anions favouring helicate formation.[16b]

Aside from these cases, interconversion of helicates and mesocates has not been reported. For the first recorded helicate/mesocate pairs, Zhang and Dolphin particularly noted that interconversion was not possible, even upon heating to high temperatures (155 °C).[14,30] For the Fe(II) mesocate incorporating the *n*-propyl spacer ligand Wu *et al.* made no mention of

Research Article
doi.org/10.1002/ejic.202200225

instability or interconversion of the mesocate in solution, and the NMR spectra indicated a single product present.[20] For the only other Ru(II) helicate/mesocate pairs reported in the literature no isomer interconversion has been noted,[11–12] making the isomer interconversion for the *n*-propyl spacer compounds a unique observation.

Two possible mechanisms were considered for the mesocate-helicate conversion.

In work by Raymond and co-workers,[14] the racemisation of digallium(III) triple-stranded helicate enantiomers ($\Delta\Delta \rightleftharpoons \Lambda\Lambda$) has been proposed to proceed by a non-dissociative Bailar[15] (or related Ray-Dutt[16]) twist in which a *meso* ($\Delta\Lambda$) intermediate is formed. The proposed *meso* intermediate, formed by the inversion at one metal centre, is considered to be of higher energy, with the spacer adopting an unfavoured conformation.[31] However, the intermediate is sufficiently accessible that the $\Delta\Delta \rightleftharpoons [\Delta\Lambda] \rightleftharpoons \Lambda\Lambda$ process occurs but its isolation was not possible, and the helicate always remains a racemate in view of the continuing inversion process. A similar mechanism for helical inversion has also been proposed by Rancan *et al.* for the racemisation of lanthanide quadruple-stranded helicates.[32] While these systems involve a thermal conversion, the principle represents one possible pathway to photo-induced isomerisation in the present system. For the Ru(II) structures containing the *n*-propyl spacer ligand, DFT calculations indicated that the mesocate and helicate forms had similar stabilities. Consequently, the conversion from $\Delta\Delta/\Lambda\Lambda \rightleftharpoons \Delta\Lambda$ may occur in the same way but the mesocate form can be observed and isolated. For this system, the *helicate*$\rightleftharpoons$*meso* interconversion does not occur thermally (*vide supra*) so that resolution of the helicate form is possible.

However, the light-induced isomerisation may instead proceed via a bond-breaking mechanism, where at least one of the Ru–N bonds at one of the Ru(II) centres must break for the inversion to occur. Photo-dissociation within Ru(II) compounds is not unknown, with the photochemical release of bpy ligands from $[Ru(bpy)_3]^{2+}$ reported both in dilute acid (at 95 °C)[33] and chlorinated solvents (at room temperature).[34] Furthermore, the photochemical release and rearrangement of ligands in mononuclear ruthenium(II) complexes containing the 4,4′-di-1,2,3-traizolyl ligand, which are structurally similar to those described above, has been described for the PF_6^- salts in acetonitrile.[35]

For the *n*-propyl spacer compounds described herein. meaningful interconversion of the two isomers was chiefly observed upon irradiation with visible light, rather than thermally, suggesting that isomerisation may proceed through a ligand dissociation pathway, similar to that proposed for mononuclear $[Ru(bpy)_3]^{2+}$ compounds. However, a twist mechanism as proposed in the racemisation of helicates, which avoids a bond-breaking process, cannot be fully discounted.

Using an *n*-butyl spacer ligand (3)

As explained above, the inclusion of an *n*-propyl spacer in the ligand resulted in a mixture of dinuclear helicate and mesocate products, indicating that it was possible to break the odd/even rules of formation for isomers of this type by combining a flexible ligand with a relatively inert metal centre, and consequently attention turned to increasing the length of the spacer further, where a mixture of isomers was again anticipated. In this case, the ligand containing an *n*-butyl spacer (**3**) was synthesised, and formation of Ru(II) compounds undertaken.

The synthesis of a triple-stranded diruthenium compound utilising the 1,4-bis{4-(pyridin-2-yl)-1*H*-1,2,3-triazol-1-yl}butane ligand (**3**) was undertaken using analogous conditions to the previously-synthesised Ru(II) compounds. The crude product was found to be composed of two major components, suggesting a mixture of dinuclear species (as had been seen for *n*-propyl spacer compounds), as well as a number of minor side products. It was found that by varying the reaction time the product distribution could be influenced (see Figure S13), and an extended reaction duration (ten hours) favoured formation of two main compounds, likely the desired dinuclear species.

Purification of the two major products isolated from the ten-hour reaction was first attempted chromatographically; however, no separation was able to be achieved using either silica or an ion-exchanger support.

The relationship of the two species was probed by a DOSY NMR experiment, which revealed that both compounds had similar diffusion coefficients, indicating that they were likely of similar sizes (see Figure S14). Given the likely presence of a mesocate and helicate pair, attention turned to exploiting the differences in chirality to separate these compounds.

Attempted separation of helicate and mesocate forms

As direct chromatographic separation of the diastereomers proved difficult, resolution of the helicate within the mixture of products was attempted. Using a cellulose solid-phase support, in conjunction with an eluent containing the chiral anion (−)-*O*,*O*′-dibenzoyl-(L)-tartrate, resolution of the helicate was achieved. The first-eluting fraction (F1) was found to contain the two species (and small quantities of impurities) by ^{1}H NMR spectroscopy, while the second-eluting fraction (F2), removed with either 0.5 M sodium 4-toluenesulfonate or 20% acetone/2 M NaCl), contained a single species (see Figure 6).

The nature of the two fractions was ascertained by CD spectroscopy, giving spectra of identical shape which were opposite in sign throughout. The first-eluting fraction (F1) had lower CD activity when adjusted for concentration, which is consistent with the NMR results showing a mixture of species present. For this sample higher absorbance was recorded by UV/Visible spectroscopy, suggesting the presence of an achiral component in the mixture, such as a mesocate. The second-eluting fraction (F2) contained a single species as shown by NMR spectroscopy and had higher relative CD intensities, indicating that this fraction must contain a resolved chiral compound, likely one hand of the purified helicate (see Figure 6). By this method resolution of the two helicate enantiomers was achieved, although the first-eluting fraction

Research Article
doi.org/10.1002/ejic.202200225

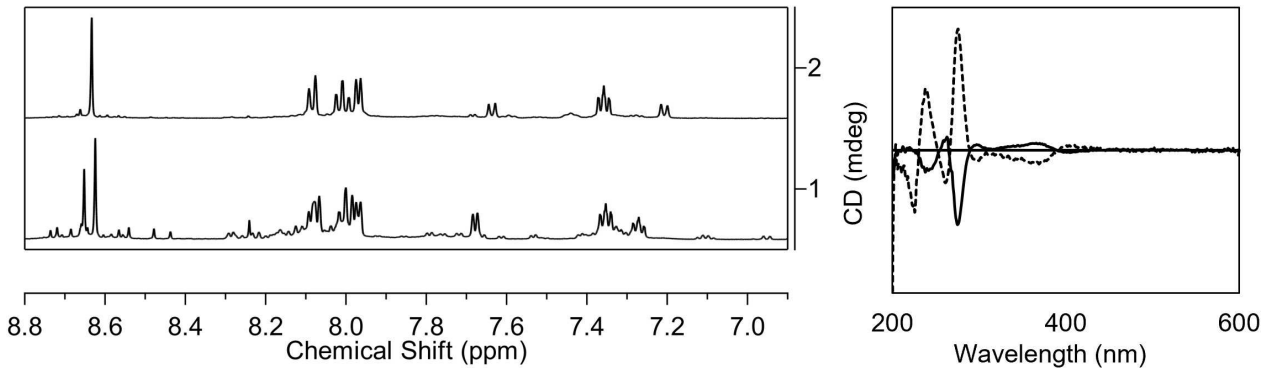

Figure 6. (LEFT) Partial ^{1}H NMR spectrum (500 MHz, CD_3CN, 298 K) and (RIGHT) CD spectrum showing the fractions from the resolution on cellulose of $[Ru_2(\mu\text{-}\mathbf{3})_3]^{4+}$: (¯) first-eluting fraction (containing a mixture of helicate/mesocate) eluted with 0.075 M sodium (−)-O,O′-dibenzoyl-(L)-tartrate; (- - - - -) second-eluting fraction (containing one enantiomer of the helicate) eluted with 0.5 M sodium 4-toluenesulfonate.

(F1) still contained a mixture of other products, thought to be chiefly the mesocate and one hand of the helicate.

For the second eluting fraction (F2) containing one enantiomer of the purified helicate, 1D and 2D NMR experiments allowed assignment of the hydrogen and carbon resonances (see Figures S15, S16, S17, S18, and S19). Following the same pattern as for the *n*-propyl spacer helicate, the hydrogens on the ligand spacer appeared as a complicated multiplet (at 4.4 ppm), and a pair of multiplets (at 1.8 ppm). The appearance of complicated multiplets for the spacer hydrogens, rather than the expected doublets, is due to the CH_2 groups becoming chemical-shift inequivalent, as well as each pair of geminal hydrogens becoming magnetically inequivalent. This has been seen for other Ru(II) mesocates,[12] such as in the work of Zhang and Dolphin,[14] and agrees with the results of Wu *et al.* for the synthesis of the Fe(II) analogues of these types of compounds, where broad multiplets corresponding to the spacer hydrogens were reported.[20]

The identity of the dinuclear species was further confirmed by HRMS, where the $\{[Ru_2\mathbf{3}_3].2PF_6\}^{2+}$ ion was present at *m/z* 766.1169 (see Figure S23). Attempts to obtain suitable crystals of the isolated F2 were unsuccessful, so the enantiomeric assignment was unable to be determined by X-ray crystallography. As a result, tentative assignment of the isolated helicate enantiomers containing the *n*-butyl spacer was attempted based on previously reported resolutions of Ru(II) compounds, as described earlier. Based on the direction of CD bands shown in Figure 6, the first-eluting fraction F1 (containing a mixture of mesocate, one helicate enantiomer, and minor side products) was proposed to contain the *P*-helicate, while the purified second-eluting fraction F2 contained the *M*-helicate.

To achieve separation of the mesocate and helicate in the first-eluting fraction a range of anions were screened for fractional crystallisation. The most promising results were seen for BF_4^-, where after two rounds of crystallisation, the precipitated sample contained predominantly the helicate (with small quantities of mesocate) with the mesocate, helicate, and unidentified minor products remaining in solution (see Figure S20).

Crystallisation of the soluble fraction (containing a mixture of species), by vapour diffusion of diisopropyl ether into a nitromethane solution of the mixture as the BF_4^- salt, provided X-ray quality crystals. This enabled a single crystal structure to be obtained, which confirmed the identity of the mesocate $[Ru_2(\mu\text{-}\mathbf{3})_3]^{4+}$ (**6**). The structure of the ruthenium(II) mesocate (**6**) is shown in Figure 7. The complex crystallises in the hexagonal space group $P6_3/m$, with half a ruthenium(II) mesocate cation and half an encapsulated nitromethane solvate guest molecule in the asymmetric unit (lying on the mirror plane). The location of the expected tetrafluoroborate anions could not be determined but, along with further solvate molecules, are presumably located in large hexagonal channels that are surrounded by columns of the mesocate structure that extend along the *c*-axis.

The two octahedral ruthenium(II) centres are separated by 9.424(2) Å, a slightly shorter distance than that recorded for the *n*-propyl spacer mesocate, and bridged by three ligands such that the stereochemistry of the metal centres of each discrete unit is ΛΔ. The four-carbon linker in the backbone of the ligand adopts an unusual eclipsed arrangement (accentuated by the disorder over the mirror plane) with all three ligands identically

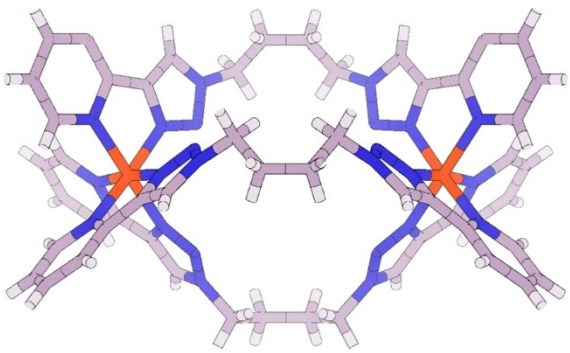

Figure 7. Crystallographic model showing the molecular structure of the ruthenium mesocate **6**, $[Ru_2(\mu\text{-}\mathbf{2})_3](PF_6)_4$. Solvent molecules and counter ions have been omitted for clarity.

Research Article
doi.org/10.1002/ejic.202200225

displaced within an individual mesocate (either clockwise or anticlockwise depending upon which end the mesocate is viewed from). The larger but squat ligand spacer provides for an internal cavity in the structure capable of including a nitromethane guest molecule, with its methyl groups surrounded by the triazole azine nitrogen atoms and the $-NO_2$ moiety directed toward the butyl spacer of the remaining ligand. Consideration of a van der Waals surface highlights the central cavity in the structure, which is occupied by a nitromethane molecule (see Figure S28).

Despite incomplete separation of the mesocate and helicate isomers (and other species), the product distribution of the dinuclear compounds was investigated using DFT calculations. The relative stability of the helicate and mesocate incorporating the *n*-butyl spacer ligand (**3**) were calculated *in vacuo* and in a dielectric medium, using the dielectric constant of acetonitrile (see Table S4). From these results it was seen that the mesocate was a more stable isomer than the helicate in acetonitrile, with $\Delta E = 16.0$ kJ/mol and $\Delta G = 7.1$ kJ/mol. This was not entirely reflected in the product distribution with the helicate being the primary product observed experimentally. The difference in stability of the two compounds was small which, in conjunction with the use of inert Ru(II) ions, may allow the formation of both isomers experimentally.

Given the challenges faced in the separation of the dinuclear Ru(II) species containing the *n*-butyl spacer ligand, no investigations into potential isomerisation were undertaken. Dinuclear compounds containing the *n*-propyl spacer ligand showed photo-isomerisation, and so it is likely that those containing the *n*-butyl spacer ligand may exhibit similar behaviour. If isomerisation does occur, it may further complicate the separation of compounds, which, coupled with the presence of multiple unknown minor products, adds another layer of complexity in predicting the product distribution for supramolecular assemblies incorporating the *n*-butyl spacer ligand.

Conclusions

This sequence of di(bidentate) ligands has been used to generate a series of triple-stranded Ru(II) helicates and mesocates. For the most rigid 1,4-xylyl spacer ligand (shortest number of sp^3 carbons) an existing helicate structure was synthesised, and resolution of the enantiomers achieved by employment of a cellulose support. By employing a relatively inert metal centre, such as Ru(II), in conjunction with ligands containing a flexible spacer, the odd/even rules of mesocate/helicate formation may be broken, allowing new supramolecular assemblies to be accessed. Of particular interest were compounds containing an *n*-propyl spacer, where the unusual isomerisation of the dinuclear assemblies was observed upon irradiation with visible light; behaviour which has not previously been reported for a mesocate/helicate pair. Increasing the spacer length, and thus flexibility of the ligand, resulted in the production of more complex product mixtures, which, while difficult to separate fully, may provide insight into the formation of larger assemblies.

Experimental Section

Materials. The ligands 1,4-bis{(4-(pyridin-2-yl)-1H-1,2,3-triazol-1-yl)methyl}benzene[17b] (**1**), 1,3-bis{4-pyridin-2-yl)-1H-1,2,3-triazol-1-yl}propane[17b] (**2**), 1,4-bis{4-(pyridin-2-yl)-1H-1,2,3-triazol-1-yl}butane[20] (**3**) and $[Ru_2(\mu\text{-}\mathbf{1})_3](PF_6)_4$[10] were synthesised by previously reported methods. All other reagents were purchased from Sigma-Aldrich and used without further purification.

General procedures and methods. High resolution mass spectrometry (HRMS) (ESI, positive-ion mode) experiments of samples dissolved in acetonitrile were performed using an Agilent Series 6230 TOF LC/MS. UV/Visible absorption spectra were acquired at ambient temperature on a Cary 1E UV-Visible Spectrophotometer (scan range: 600–200 nm, scan rate: 600.00 nm/min, SBW: 2.0 nm). Circular dichroism (CD) spectra were measured at ambient temperature using a Jasco J-715 spectropolarimeter (scan range: 600–200 nm, resolution: 1 nm, bandwidth: 2.0 nm, sensitivity: 200 mdeg, response: 1 sec, speed: 100 nm/min). Scanning Electron Microscope (SEM) images were collected on a Quanta 450 scanning electron microscope in secondary electron mode (spot size 4 and 15 KeV). Samples for SEM analysis were wet loaded onto adhesive carbon tabs and carbon coated (5 nm) prior to analysis. Electron Dispersive X-ray Analysis was collected with an Oxford Instruments Ultim Max 170 EDX attachment on the Quanta 450. All ^{1}H NMR and ^{13}C NMR spectra were obtained using an Agilent 500 MHz NMR spectrometer operating at 500/126 MHz or a Varian Inova operating at 600/151 MHz at 25 °C, unless otherwise stated. Spectra of samples were recorded in solutions of $CDCl_3$, using TMS as an internal standard, CD_3CN, d_6-DMSO, or D_2O. The following abbreviations for hydrogen multiplicities were used: s, singlet; d, doublet; t, triplet; m, multiplet; and br, broad. ^{1}H signals were assigned with assistance of 2D NMR experiments where required. Experiments under microwave irradiation were performed with a CEM microwave reactor at 225 °C (power 200 W, pressure 200 psi) for five or ten hours. All compounds were anion exchanged using Dowex 1X-8 (Cl) 20–50 mesh to form the chloride salts. Cellulose chromatography was performed using Aldrich (20 micron) microcrystalline cellulose powder.

Syntheses

$[Ru_2(\mu\text{-}\mathbf{2})_3](PF_6)_4$ mesocate (4) and helicate (5)

A solution of $RuCl_3 \cdot 3H_2O$ (41 mg, 0.2 mmol; 2 equiv.) and 1,3-bis{4-pyridin-2-yl)-1H-1,2,3-triazol-1-yl}propane (**2**; 100 mg, 0.3 mmol; 3 equiv.) in ethylene glycol (16 mL) was irradiated in a CEM microwave reactor at 225 °C (power 200 W, pressure 200 psi) for 5 h. The solution was cooled to room temperature, deionised water added (20 mL), and the mixture filtered through Celite. An aqueous solution of KPF_6 (4%, 5 mL) was added to the filtrate, and the resulting precipitate isolated by centrifugation (10621 g, 5 min), washed with water, and dried under vacuum to give the crude product, as a yellow powder. The crude product was exchanged to the Cl^- salt (Dowex 1-X8) in H_2O, the resulting yellow solution filtered, and solvent removed. Partial dissolution of the resulting solid in DMSO allowed separation of the mesocate and helicate, where the mesocate was precipitated, while the helicate remained in solution. The DMSO precipitate was collected by centrifugation (10621 g, 20 min), washed vigorously with DMSO (20 mL), and dissolved in H_2O. Aqueous KPF_6 (4%, 5 mL) was added, and the resulting precipitate isolated by centrifugation (10621 g, 5 min),

washed with water, and dried under vacuum to give the mesocate (**4**), as a yellow powder (0.11 g, 32%). X-ray quality crystals were grown by vapour diffusion of diisopropyl ether into a nitromethane solution of the compound as the PF_6^- salt. λ_{max} CH_3CN/nm (ε/$M^{-1}cm^{-1}$) 382 (2.46×10^4), 268 (1.06×10^5), 237 (2.55×10^4). δ_H (500 MHz, CD_3CN) 8.61 (s, 1H), 8.10 (d, J = 7.5 Hz, 1H), 8.04–7.96 (m, 2H), 7.37 (t, J = 6.1 Hz, 1H), 4.48–4.33 (m, 2H), 2.61–2.35 (m, 1H). δ_C (126 MHz, CD_3CN) 153.36, 152.37, 148.14, 142.25, 139.22, 126.78, 125.93, 123.18, 49.77, 31.75. m/z (ESI) 300.0639 {[Ru_2(**2**)$_3$].4PF_6}. The DMSO solution was diluted with H_2O (100 mL) and aqueous KPF_6 (4%, 5 mL) added. The resulting precipitate was isolated by centrifugation (10621 g, 5 min), washed with water, and dried under vacuum to give the helicate (**5**), as a yellow powder (0.14 g, 40%). X-ray quality crystals were grown by vapour diffusion of diisopropyl ether into an acetonitrile solution of the compound as the PF_6^- salt. λ_{max} CH_3CN/nm (ε/$M^{-1}cm^{-1}$) 382 (3.17×10^4), 268 (1.39×10^5), 233 (3.17×10^4). δ_H (500 MHz, CD_3CN) 8.63 (s, 1H), 8.10 (d, J = 7.7 Hz, 1H), 8.02 (td, J = 7.8, 1.4 Hz, 1H), 7.97 (d, J = 5.6 Hz, 1H), 7.37 (ddd, J = 7.4, 5.7, 1.4 Hz, 1H), 4.51–4.42 (m, 1H), 4.33–4.23 (m, 2H), 2.62–2.55 (m, 1H). δ_C (126 MHz, CD_3CN) 153.29, 152.40, 148.34, 139.16, 126.74, 125.86, 123.12, 49.59, 28.79. m/z (ESI) 300.0651 {[Ru_2(**2**)$_3$].4PF_6}.

*[Ru_2(μ-**3**)$_3$](PF_6)$_4$ (**6**)*

A solution of $RuCl_3\cdot3H_2O$ (39 mg, 0.19 mmol; 2 equiv.) and 1,4-bis {4-(pyridin-2-yl)-1H-1,2,3-triazol-1-yl}butane (**3**; 100 mg, 0.29 mmol; 3 equiv.) in ethylene glycol (16 mL) was irradiated in a CEM microwave reactor at 225 °C (power 200 W, pressure 200 psi) for 5 or 10 h. The solution was cooled to room temperature, deionised water added (20 mL), and the mixture filtered through Celite. An aqueous solution of KPF_6 (4%, 5 mL) was added to the filtrate, and the resulting precipitate isolated by centrifugation (10621 g, 5 min), washed with water, and dried under vacuum to give the crude product, as a yellow powder. The crude product was exchanged to the Cl^- salt (Dowex 1-X8) in H_2O, the resulting yellow solution filtered, and concentrated by removal of solvent. Cellulose was mixed with H_2O to form a slurry and then packed onto a column of ~100 mm length, 10 mm diameter. The concentrated aqueous solution containing the crude Ru(II) product mixture was loaded onto the column and eluted with aqueous 0.075 M sodium (−)-*O,O′*-dibenzoyl-L-tartrate, and the single eluting band collected. The column was then washed with 0.5 M sodium 4-toluenesulfonate/(20% acetone/2 M NaCl) to collect the remaining retained compound. To remove the chiral anions both solutions were individually passed through a small column of silica gel and washed with copious amounts of acetone and water. Each fraction was then removed from the silica by elution with a solution of NH_4PF_6 in acetone (4%). Water (1 mL) was added to the eluate and the acetone removed by rotary evaporation. In each case the resulting solid was collected by centrifugation (10621 g, 5 min), washed with cold water (3x), and dried under vacuum. The product from the first eluted fraction (F1), containing a mixture of mesocate and one enantiomer of the helicate, was then exchanged to the Cl^- salt (Dowex 1-X8) in H_2O and the resulting yellow solution filtered. An aqueous solution of 0.5 M $NaBF_4$ was added to the aqueous crude product Cl^- solution in a dropwise manner, until precipitation was observed. The solution was cooled to 5 °C for 24 h, and the resulting yellow precipitate filtered. The yellow precipitate (from two rounds of crystallisation with BF_4^-) was washed with water and dried to give a purified mixture of mesocate and helicate as the BF_4^- salt. The compound remaining in solution (from two rounds of crystallisation with BF_4^-) was isolated as the PF_6^- salt by addition of an aqueous solution of KPF_6 (4%, 5 mL). The resulting solid (as the PF_6^- salt) was isolated by centrifugation (10621 g, 5 min), washed with cold water, and dried under vacuum to give a complex mixture of dinuclear species and unknown side products, as a yellow powder. Crystallisation of the soluble fraction (containing a mixture of species), by vapour diffusion of diisopropyl ether into a nitromethane solution of the mixture as the BF_4^- salt, provided X-ray quality crystals of the mesocate (**6**). The second eluted fraction from the resolution on cellulose (F2), was isolated as the PF_6^- salt and found to contain a single enantiomer of the helicate (**7**), as a yellow powder. λ_{max} CH_3CN/nm (ε/$M^{-1}cm^{-1}$) 382 (3.17×10^4), 268 (1.39×10^5), 233 (3.17×10^4). δ_H (599 MHz, CD_3CN) 8.63 (s, 1H), 8.08 (d, J = 7.9 Hz, 1H), 8.01 (td, J = 7.8, 1.4 Hz, 1H), 7.97 (d, J = 5.5 Hz, 1H), 7.35 (ddd, J = 7.3, 5.7, 1.4 Hz, 1H), 4.41–4.27 (m, 1H), 4.33–4.23 (m, 2H), 1.86–1.67 (m, 2H). δ_C (126 MHz, CD_3CN) 153.19, 152.27, 148.86, 139.03, 126.64, 125.60, 123.04, 52.21, 27.27. m/z (ESI) {[Ru_2**3**$_3$]}$^{4+}$.

Crystal data and structure refinement for the purified complexes **5**, **6** and **7** are given in Table S1.

*Resolution of [Ru_2(μ-**1**)$_3$]$^{4+}$*

Cellulose was mixed with H_2O to form a slurry and then packed onto a column of ~100 mm length, 10 mm diameter. A concentrated aqueous solution containing a racemic mixture of [Ru_2(μ-**1**)$_3$]$^{4+}$ was loaded and the column eluted with aqueous 2 M NaCl solution, yielding an eluate (F1) containing the *M*-helicate. The residual material on the column was then washed with 0.5 M sodium 4-toluenesulfonate or 20% acetone/2 M NaCl allowing elution of the *P*-helicate (F2). To remove the chiral anions both solutions were individually passed through a small column of silica gel and washed with copious amounts of acetone and water. Each fraction was then removed from the silica by elution with a solution of NH_4PF_6 in acetone (4%). Water (1 mL) was added and the acetone removed by rotary evaporation. In each case the resulting solid was collected by centrifugation (10621 g, 5 min), washed with cold water (3x), and dried under vacuum.

Computational Studies. For each Ru(II) compound, density functional theory (DFT) calculations were performed with Q-Chem version 5.1,[36] using helicate or mesocate structural data from the experimental X-ray crystal structures. In cases where the crystal structure was not available, existing crystal structures containing other transition metal centres, or ligands, were modified to allow modelling of theoretical supramolecular assemblies. All geometries were optimised at the ωB97X-D/SRSC level[37] *in vacuo*. Harmonic frequencies were calculated for the optimised geometries *in vacuo* at the same level of theory. The single-point energy was calculated for each optimised geometry at the ωB97X-D/SRSC level in a dielectric medium using the CPCM method[38] and the dielectric constant of acetonitrile (35.85).[39] The Bondi radius for ruthenium of 2.05 Å was taken from Alvarez *et al.*,[40] and multiplied by 1.2 as per Q-Chem default, to give 2.46 Å. The difference in Gibbs free energy, ΔG, between two structures was calculated from the difference in energy, ΔE, by adding $\Delta H_{thermal} - T\Delta S_{thermal}$, where $\Delta H_{thermal}$ and $\Delta S_{thermal}$ are the differences in the thermal (translational, rotational, and vibrational) corrections to the enthalpy and entropy, respectively, at temperature $T = 298.15$ K and pressure = 1 atm. Default parameters were used in all cases except for SCF convergence in geometry and frequency calculations, which was set to 10^{-7} instead of 10^{-8} due to difficulties in convergence.

Deposition Numbers 2165030 (for **4**), 2165029 (for **5**), and 2165031 (for **6**) contain the supplementary crystallographic data for this paper. These data are provided free of charge by the joint Cambridge Crystallographic Data Centre and Fachinformationszentrum Karlsruhe Access Structures service www.ccdc.cam.ac.uk/structures.

Acknowledgements

The authors acknowledge the instruments and scientific and technical assistance of Microscopy Australia at Adelaide Microscopy, The University of Adelaide, a facility that is funded by the University, and State and Federal Governments. Aspects of this research were undertaken on the MX1 and MX2 beamlines at the Australian Synchrotron, Victoria, Australia. This work was supported with supercomputing resources provided by the Phoenix HPC service at the University of Adelaide. Open access publishing facilitated by The University of Adelaide, as part of the Wiley - The University of Adelaide agreement via the Council of Australian University Librarians.

Conflict of Interest

The authors declare no conflict of interest.

Data Availability Statement

The data that support the findings of this study are available in the supplementary material of this article.

Keywords: Density functional calculations · Helical structures · Photochemistry · Ruthenium · Supramolecular chemistry

[1] a) E. Yashima, N. Ousaka, D. Taura, K. Shimomura, T. Ikai, K. Maeda, *Chem. Rev.* **2016**, *116*, 13752–13990; b) C. Piguet, G. Bernardinelli, G. Hopfgartner, *Chem. Rev.* **1997**, *97*, 2005–2062; c) M. J. Hannon, L. J. Childs, *Supramol. Chem.* **2004**, *16*, 7–22.

[2] a) A. K. Gorle, A. J. Ammit, L. Wallace, F. R. Keene, J. G. Collins, *New J. Chem.* **2014**, *38*, 4049–4059; b) X. Li, A. K. Gorle, M. K. Sundaraneedi, F. R. Keene, J. G. Collins, *Coord. Chem. Rev.* **2018**, *375*, 134–147.

[3] a) F. Li, J. G. Collins, F. R. Keene, *Chem. Soc. Rev.* **2015**, *44*, 2529–2542; b) A. Bolhuis, L. Hand, J. E. Marshall, A. D. Richards, A. Rodger, J. Aldrich-Wright, *Eur. J. Pharm. Sci.* **2011**, *42*, 313–317; c) A.-C. Munteanu, V. Uivarosi, *Pharmaceutica* **2021**, *13*, 874.

[4] a) J. J. Silva, P. M. Guedes, A. Zottis, T. L. Balliano, F. O. Nascimento Silva, L. G. França Lopes, J. Ellena, G. Oliva, A. D. Andricopulo, D. W. Franco, J. S. Silva, *Br. J. Pharmacol.* **2010**, *160*, 260–269; b) M. K. Sundaraneedi, B. A. Tedla, R. M. Eichenberger, L. Becker, D. Pickering, M. J. Smout, S. Rajan, P. Wangchuk, F. R. Keene, A. Loukas, J. G. Collins, M. S. Pearson, *PLoS Neglected Trop. Dis.* **2017**, *11*, e0006134; c) M. Sundaraneedi, R. M. Eichenberger, R. Al-Hallaf, D. Yang, J. Sotillo, S. Rajan, P. Wangchuk, P. R. Giacomin, F. R. Keene, A. Loukas, J. G. Collins, M. S. Pearson, *Int. J. Parasitol.: Drugs Drug Resist.* **2018**, *8*, 1–7.

[5] Y. Lin, H. Betts, S. Keller, K. Cariou, G. Gasser, *Chem. Soc. Rev.* **2021**, *50*, 10346–10402.

[6] J. D. Crane, J.-P. Sauvage, *New J. Chem.* **1992**, *16*, 649–650.

[7] G. I. Pascu, A. C. G. Hotze, C. Sanchez-Cano, B. M. Kariuki, M. J. Hannon, *Angew. Chem. Int. Ed.* **2007**, *46*, 4374–4378; *Angew. Chem.* **2007**, *119*, 4452–4456.

[8] a) J. Malina, M. J. Hannon, V. Brabec, *Chem. Eur. J.* **2008**, *14*, 10408–10414; b) C. Ducani, A. Leczkowska, N. J. Hodges, M. J. Hannon, *Angew. Chem. Int. Ed.* **2010**, *49*, 8942–8945; *Angew. Chem.* **2010**, *122*, 9126–9129; c) L. Cardo, I. Nawroth, P. J. Cail, J. A. McKeating, M. J. Hannon, *Sci. Rep.* **2018**, *8*, 13342.

[9] C. R. K. Glasson, G. V. Meehan, J. K. Clegg, L. F. Lindoy, J. A. Smith, F. R. Keene, C. Motti, *Chem. Eur. J.* **2008**, *14*, 10535–10538.

[10] S. V. Kumar, W. K. C. Lo, H. J. L. Brooks, J. D. Crowley, *Inorg. Chim. Acta* **2015**, *425*, 1–6.

[11] S. J. Allison, D. Cooke, F. S. Davidson, P. I. P. Elliott, R. A. Faulkner, H. B. S. Griffiths, O. J. Harper, O. Hussain, P. J. Owen-Lynch, R. M. Phillips, C. R. Rice, S. L. Shepherd, R. T. Wheelhouse, *Angew. Chem. Int. Ed.* **2018**, *57*, 9799–9804; *Angew. Chem.* **2018**, *130*, 9947–9952.

[12] K. L. Flint, J. G. Collins, S. J. Bradley, T. A. Smith, C. J. Sumby, F. R. Keene, *Aust. J. Chem.* **2019**, *72*, 762–768.

[13] M. Albrecht, S. Kotila, *Angew. Chem. Int. Ed.* **1995**, *34*, 2134–2137; *Angew. Chem.* **1995**, *107*, 2285–2287.

[14] Z. Zhang, D. Dolphin, *Chem. Commun.* **2009**, 6931–6933.

[15] a) M. Albrecht, *Chem. Rev.* **2001**, *101*, 3457–3497; b) Z. Zhang, Y. Chen, D. Dolphin, *Dalton Trans.* **2012**, *41*, 4751–4753.

[16] a) S. Goetz, P. E. Kruger, *Dalton Trans.* **2006**, 1277–1284; b) F. J. Cui, S. G. Li, C. D. Jia, J. S. Mathieson, L. Cronin, X. J. Yang, B. Wu, *Inorg. Chem.* **2012**, *51*, 179–187.

[17] a) J. D. Crowley, S. M. Goldup, A.-L. Lee, D. A. Leigh, R. T. McBurney, *Chem. Soc. Rev.* **2009**, *38*, 1530–1541; b) J. D. Crowley, P. H. Bandeen, *Dalton Trans.* **2010**, *39*, 612–623; c) J. D. Crowley, D. A. McMorran, in *Click Triazoles* (Ed.: J. Košmrlj), Springer Berlin Heidelberg, Berlin, Heidelberg, **2012**, pp. 31–83; d) Q. V. C. van Hilst, N. R. Lagesse, D. Preston, J. D. Crowley, *Dalton Trans.* **2018**, *47*, 997–1002.

[18] R. A. Vasdev, D. Preston, S. O. Scottwell, H. J. Brooks, J. D. Crowley, M. P. Schramm, *Molecules* **2016**, *21*.

[19] S. K. Vellas, J. E. M. Lewis, M. Shankar, A. Sagatova, J. D. A. Tyndall, B. C. Monk, C. M. Fitchett, L. R. Hanton, J. D. Crowley, *Molecules* **2013**, *18*, 6383–6407.

[20] N. Wu, C. F. C. Melan, K. A. Stevenson, O. Fleischel, H. Guo, F. Habib, R. J. Holmberg, M. Murugesu, N. J. Mosey, H. Nierengarten, A. Petitjean, *Dalton Trans.* **2015**, *44*, 14991–15005.

[21] M. Albrecht, *Chem. Eur. J.* **2000**, *6*, 3485–3489.

[22] S. V. Kumar, S. O. Scottwell, E. Waugh, C. J. McAdam, L. R. Hanton, H. J. Brooks, J. D. Crowley, *Inorg. Chem.* **2016**, *55*, 9767–9777.

[23] K. A. Stevenson, C. F. C. Melan, O. Fleischel, R. Y. Wang, A. Petitjean, *Cryst. Growth Des.* **2012**, *12*, 5169–5173.

[24] a) A. M. Najar, C. Avci, M. D. Ward, *Inorg. Chem. Commun.* **2012**, *15*, 126–129; b) U. R. Pokharel, J. C. Theriot, F. R. Fronczek, A. W. Maverick, *Polyhedron* **2020**, *191*, 114805.

[25] a) M. J. Hannon, I. Meistermann, C. J. Isaac, C. Blomme, J. R. Aldrich-Wright, A. Rodger, *Chem. Commun.* **2001**, 1078–1079; b) J. Kerckhoffs, J. C. Peberdy, I. Meistermann, L. J. Childs, C. J. Isaac, C. R. Pearmund, V. Reudegger, S. Khalid, N. W. Alcock, M. J. Hannon, A. Rodger, *Dalton Trans.* **2007**, 734–742; c) A. Leczkowska, PhD thesis, The University of Birmingham **2011**.

[26] A. J. McCaffery, S. F. Mason, B. J. Norman, *J. Chem. Soc. A* **1969**, 1428–1441.

[27] H. Crlikova, J. Malina, V. Novohradsky, H. Kostrhunova, R. A. S. Vasdev, J. D. Crowley, J. Kasparkova, V. Brabec, *Organometallics* **2020**, *39*, 1448–1455.

[28] J. B. Maglic, R. Lavendomme, *ChemRxiv* **2021**, DOI 10.26434/chemrxiv-2021-dss1j. This content is a preprint and has not been peer-reviewed.

[29] a) M. Scherer, D. L. Caulder, D. W. Johnson, K. N. Raymond, *Angew. Chem. Int. Ed.* **1999**, *38*, 1587–1592; *Angew. Chem.* **1999**, *111*, 1689–1694; b) P. N. W. Baxter, J.-M. Lehn, G. Baum, D. Fenske, *Chem. Eur. J.* **2000**, *6*, 4510–4517; c) I. A. Riddell, Y. R. Hristova, J. K. Clegg, C. S. Wood, B. Breiner, J. R. Nitschke, *J. Am. Chem. Soc.* **2013**, *135*, 2723–2733; d) B. Li, W. Zhang, S. Lu, B. Zheng, D. Zhang, A. Li, X. Li, X.-J. Yang, B. Wu, *J. Am. Chem. Soc.* **2020**, *142*, 21160–21168; e) D. A. Roberts, B. S. Pilgrim, G. Sirvinskaite, T. K. Ronson, J. R. Nitschke, *J. Am. Chem. Soc.* **2018**, *140*, 9616–9623; f) X. Bai, C. Jia, Y. Zhao, D. Yang, S.-C. Wang, A. Li, Y.-T. Chan, Y.-Y. Wang, X.-J. Yang, B. Wu, *Angew. Chem. Int. Ed.* **2018**, *57*, 1851–1855; *Angew. Chem.* **2018**, *130*, 1869–1873.

[30] Z. Zhang, D. Dolphin, *Inorg. Chem.* **2010**, *49*, 11550–11555.

[31] M. Albrecht, I. Janser, H. Houjou, R. Fröhlich, *Chem. Eur. J.* **2004**, *10*, 2839–2850.

[32] M. Rancan, J. Tessarolo, A. Carlotto, S. Carlotto, M. Rando, L. Barchi, E. Bolognesi, R. Seraglia, G. Bottaro, M. Casarin, G. H. Clever, L. Armelao, *Cell Rep. Phys. Sci.* **2022**, *3*, 100692.

[33] J. Van Houten, R. J. Watts, *Inorg. Chem.* **1978**, *17*, 3381–3385.

[34] a) M. Gleria, F. Minto, G. Beggiato, P. Bortolus, *J. Chem. Soc. Chem. Commun.* **1978**, 285a–285a; b) B. Durham, J. V. Caspar, J. K. Nagle, T. J. Meyer, *J. Am. Chem. Soc.* **1982**, *104*, 4803–4810; c) A. Yamagishi, K. Naing, Y. Goto, M. Taniguchi, M. Takahashi, *J. Chem. Soc. Dalton Trans.* **1994**, 2085–2089.

[35] a) P. A. Scattergood, U. Khushnood, A. Tariq, D. J. Cooke, C. R. Rice, P. I. P. Elliott, *Inorg. Chem.* **2016**, *55*, 7787–7796; b) I. M. Dixon, J.-L.

Heully, F. Alary, P. I. P. Elliott, *Phys. Chem. Chem. Phys.* **2017**, *19*, 27765–27778.

[36] Y. Shao, Z. Gan, E. Epifanovsky, A. T. B. Gilbert, M. Wormit, J. Kussmann, A. W. Lange, A. Behn, J. Deng, X. Feng, D. Ghosh, M. Goldey, P. R. Horn, L. D. Jacobson, I. Kaliman, R. Z. Khaliullin, T. Kuś, A. Landau, J. Liu, E. I. Proynov, Y. M. Rhee, R. M. Richard, M. A. Rohrdanz, R. P. Steele, E. J. Sundstrom, H. L. Woodcock III, P. M. Zimmerman, D. Zuev, B. Albrecht, E. Alguire, B. Austin, G. J. O. Beran, Y. A. Bernard, E. Berquist, K. Brandhorst, K. B. Bravaya, S. T. Brown, D. Casanova, C.-M. Chang, Y. Chen, S. H. Chien, K. D. Closser, D. L. Crittenden, M. Diedenhofen, R. A. D. Jr, H. Do, A. D. Dutoi, R. G. Edgar, S. Fatehi, L. Fusti-Molnar, A. Ghysels, A. Golubeva-Zadorozhnaya, J. Gomes, M. W. D. Hanson-Heine, P. H. P. Harbach, A. W. Hauser, E. G. Hohenstein, Z. C. Holden, T.-C. Jagau, H. Ji, B. Kaduk, K. Khistyaev, J. Kim, J. Kim, R. A. King, P. Klunzinger, D. Kosenkov, T. Kowalczyk, C. M. Krauter, K. U. Lao, A. D. Laurent, K. V. Lawler, S. V. Levchenko, C. Y. Lin, F. Liu, E. Livshits, R. C. Lochan, A. Luenser, P. Manohar, S. F. Manzer, S.-P. Mao, N. Mardirossian, A. V. Marenich, S. A. Maurer, N. J. Mayhall, E. Neuscamman, C. M. Oana, R. Olivares-Amaya, D. P. O'Neill, J. A. Parkhill, T. M. Perrine, R. Peverati, A. Prociuk, D. R. Rehn, E. Rosta, N. J. Russ, S. M. Sharada, S. Sharma, D. W. Small, A. Sodt, T. Stein, D. Stück, Y.-C. Su, A. J. W. Thom, T. Tsuchimochi, V. Vanovschi, L. Vogt, O. Vydrov, T. Wang, M. A. Watson, J. Wenzel, A. White, C. F. Williams, J. Yang, S. Yeganeh, S. R. Yost, Z.-Q. You, I. Y. Zhang, X. Zhang, Y. Zhao, B. R. Brooks, G. K. L. Chan, D. M. Chipman, C. J. Cramer, W. A. Goddard III, M. S. Gordon, W. J. Hehre, A. Klamt, H. F. Schaefer III, M. W. Schmidt, C. D. Sherrill, D. G. Truhlar, A. Warshel, X. Xu, A. Aspuru-Guzik, R. Baer, A. T. Bell, N. A. Besley, J.-D. Chai, A. Dreuw, B. D. Dunietz, T. R. Furlani, S. R. Gwaltney, C.-P. Hsu, Y. Jung, J. Kong, D. S. Lambrecht, W. Liang, C. Ochsenfeld, V. A. Rassolov, L. V. Slipchenko, J. E. Subotnik, T. V. Voorhis, J. M. Herbert, A. I. Krylov, P. M. W. Gill, M. Head-Gordon, *Mol. Phys.* **2015**, *113*, 184.

[37] a) J.-D. Chai, M. Head-Gordon, *J. Chem. Phys.* **2008**, *128*, 084106; b) J.-D. Chai, M. Head-Gordon, *Phys. Chem. Chem. Phys.* **2008**, *10*, 6615–6620.

[38] a) M. Cossi, N. Rega, G. Scalmani, V. Barone, *J. Comput. Chem.* **2003**, *24*, 669–681; b) J. Tomasi, B. Mennucci, R. Cammi, *Chem. Rev.* **2005**, *105*, 2999–3094.

[39] J.-F. Côté, D. Brouillette, J. E. Desnoyers, J.-F. Rouleau, J.-M. St-Arnaud, G. Perron, *J. Solution Chem.* **1996**, *25*, 1163–1173.

[40] S. Alvarez, *Dalton Trans.* **2013**, *42*, 8617–8636.

Manuscript received: April 12, 2022
Revised manuscript received: May 22, 2022
Accepted manuscript online: May 23, 2022

RESEARCH ARTICLE

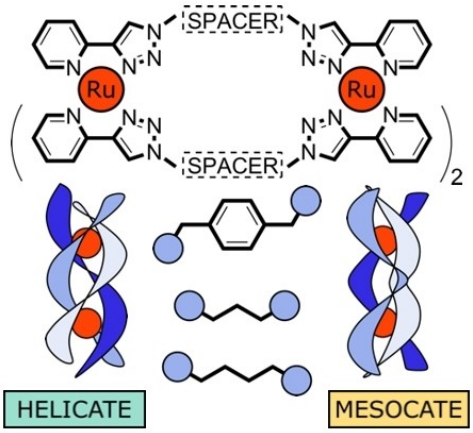

*Dr. K. L. Flint, Dr. D. M. Huang, Dr. O. M. Linder-Patton, Prof. C. J. Sumby, Prof. F. R. Keene**

The product distribution in dinuclear Ru(II) triple-stranded complexes was influenced by modifying the length and flexibility of the ligands, allowing previously unexplored helicate/mesocate pairs to be accessed. Full or partial resolution of the enantiomers of helicate products was achieved, and photoisomerism of one pair of diastereomers was observed.